metals

Article

Effect of Manganese on the Structure-Properties Relationship of Cold Rolled AHSS Treated by a Quenching and Partitioning Process

Simone Kaar [1,*], Daniel Krizan [2], Reinhold Schneider [1], Coline Béal [3] and Christof Sommitsch [3]

1 Research and Development, University of Applied Sciences Upper Austria, Wels 4600, Austria; reinhold.schneider@fh-wels.at
2 Research and Development Department, Business Unit Coil, voestalpine Stahl GmbH, Linz 4020, Austria; daniel.krizan@voestalpine.com
3 Institute of Materials Science, Joining and Forming, Graz University of Technology, Graz 8010, Austria; coline.beal@tugraz.at (C.B.); christof.sommitsch@tugraz.at (C.S.)
* Correspondence: simone.kaar@fh-wels.at; Tel.: +43-50304-15-6250

Received: 17 September 2019; Accepted: 16 October 2019; Published: 19 October 2019

Abstract: The present work focuses on the investigation of both microstructure and resulting mechanical properties of different lean medium Mn Quenching and Partitioning (Q&P) steels with 0.2 wt.% C, 1.5 wt.% Si, and 3–4 wt.% Mn. By means of dilatometry, a significant influence of the Mn-content on their transformation behavior was observed. Light optical and scanning electron microscopy (LOM, SEM) was used to characterize the microstructure consisting of tempered martensite (α''), retained austenite (RA), partially bainitic ferrite (α_B), and final martensite (α'_{final}) formed during final cooling to room temperature (RT). Using the saturation magnetization measurements (SMM), a beneficial impact of the increasing Mn-content on the volume fraction of RA could be found. This remarkably determined the mechanical properties of the investigated steels, since the larger amount of RA with its lower chemical stabilization against the strain-induced martensite transformation (SIMT) highly influenced their overall stress-strain behavior. With increasing Mn-content the ultimate tensile strength (UTS) rose without considerable deterioration in total elongation (TE), leading to an enhanced combination of strength and ductility with UTS × TE exceeding 22,500 MPa%. However, for the steel grades containing an elevated Mn-content, a narrower process window was observed due to the tendency to form α'_{final}.

Keywords: lean medium Mn Q&P steel; stress-strain behavior; mechanical properties; retained austenite stability

1. Introduction

Increasing requirements of the automotive industry related to lightweight construction and increased passenger safety drive the development of advanced high strength steels (AHSS) [1,2]. Currently, research focuses on the development of the third generation AHSS, including the concepts of medium Mn and Quenching and Partitioning (Q&P) steels. These steel grades offer a promising combination of strength and ductility achieved by a microstructure having a substantial amount of retained austenite (RA) which transforms into strain-induced martensite (α') due to the transformation induced plasticity (TRIP) effect [3–5].

Medium Mn steels with a typical chemical composition of 0.05–0.2 wt.% C and 3–10 wt.% Mn have a microstructure consisting of an ultrafine-grained ferritic (α) matrix and volume fractions of retained austenite (RA) up to 40 vol.%. Therefore, they are characterized by an excellent combination of strength and ductility, achieving ultimate tensile strengths (UTS) > 800 MPa combined with total elongations (TE) of up to 40% [6–8].

Q&P is being considered as a novel heat treatment to produce steels with a carbon-depleted α″ matrix that contain a considerable volume fraction of RA. The Q&P process was first proposed by Speer et al. [9], and consists of a two-step heat treatment. After heating in order to obtain a fully austenitic microstructure, the steel is initially quenched to a specific quenching temperature (T_Q) in the M_S-M_f temperature range, where austenite partially transforms into primary martensite (α'_{prim}). In a second step, the steel is reheated to the so-called partitioning temperature (T_P), where carbon diffuses from the supersaturated α'_{prim} into the untransformed austenite, resulting in its appropriate stabilization upon final cooling to RT [9,10]. In order to ensure the retention of the largest RA fraction, the formation of carbides has to be avoided as much as possible. The addition of Si, Al, or P allows the suppression of cementite precipitation during isothermal holding at T_P, since these elements are considered to be insoluble in cementite [11]. Thus, the cementite growth requires the time-consuming rejection of Si, Al, or P, leading to its postponed precipitation, hence enabling the carbon to partition into austenite. Furthermore, the ε or η transition carbides are known to precipitate already during quenching to T_Q or in the early stages of the partitioning step. However, unlike the influence on cementite formation, the effect of Si, Al, and P on the formation of transition carbides is less clear [12]. From the current research perspective, alloying with these elements does not effectively suppress the precipitation of transition carbides, since they seem to be able to incorporate these elements as solutes [13,14].

The application of the Q&P process to lean medium Mn steels has already been investigated in several studies [15–18]. A beneficial influence of an increased Mn-content on the volume fraction of RA of Q&P steels was confirmed by De Moor [15] and Seo et al. [17]. De Moor et al. [16] has compared the tensile behavior of two 0.3C-3Mn-1.6Si and 0.3C-5Mn-1.6Si steel grades subjected to Q&P heat-treatment and could not state a positive influence of the increased Mn-content on the mechanical properties due to the presence of final martensite in the microstructure of the steel grade containing an elevated Mn level. However, an excellent combination of strength and ductility with UTS × TE exceeding 25,000 MPa was found by Seo et al. [18] for a 0.2C-4.0Mn-1.6Si-1.0Cr Q&P steel.

Since there is still a lack of information regarding the influence of the Mn-content for Q&P steels, this work focuses on the comparison of the microstructure and resulting mechanical properties of three different lean medium Mn Q&P steels containing 0.2 wt.% C, 3.0–4.0 wt.% Mn, and 1.5 wt.% Si. By varying T_Q, the volume fraction of α'_{prim} and thus, RA and α_B were adjusted in order to enable a detailed characterization of the microstructural development and the resulting mechanical properties. Furthermore, since it is not solely the volume fraction of RA, which determines the tensile behavior of TRIP-assisted AHSS, but rather its stabilization against the strain-induced martensite transformation (SIMT), the RA-stability was examined in detail and linked to the stress-strain behavior of the investigated steel grades.

2. Materials and Methods

The chemical compositions of the investigated steel grades with varying Mn-contents are given in Table 1. Three 80 kg ingots were cast under laboratory conditions in a medium frequency furnace, followed by hot rolling to a final thickness of 4 mm. In order to provide cold rollability, the hot rolled sheets (finish rolling temperature = 900 °C) were tempered in a batch-annealing-like furnace for 16 h at 550 °C. Subsequently, the material was cold rolled to a final thickness of 1 mm.

Table 1. Chemical composition of the investigated cold rolled steel grades.

Steel	C	Mn	Si
Fe-C-3.0Mn-Si	0.20	3.06	1.52
Fe-C-3.5Mn-Si	0.20	3.47	1.51
Fe-C-4.0Mn-Si	0.20	3.94	1.50

Specimens of 10 × 4 × 1 mm^3 were heat-treated on a Bähr 805 A/D dilatometer (TA instruments, New Castle, DE, USA) in order to investigate the influence of both, T_Q and Mn-content on the transformation behavior of the cold rolled sheets. Figure 1 shows the applied time-temperature schedules for the Q&P process, adapted to suit an industrially feasible continuous annealing line. After full austenitization for t_A = 120 s at T_A = 850 °C the samples were quenched to various T_Q in the range of 130–330 °C with a 20 °C step and isothermally held for 10 s (t_Q). Subsequently, partitioning was performed at T_P = 400 °C for 300 s, followed by cooling to RT. For tensile testing, strips of 450 × 20 × 1 mm^3 were heat-treated referring to the equal time-temperature regime using a multipurpose annealing simulator (MULTIPAS, voestalpine Stahl GmbH, Linz, Austria), providing electrical resistance heating and gas jet cooling. Three thermocouples were welded onto the strip in order to ensure temperature control.

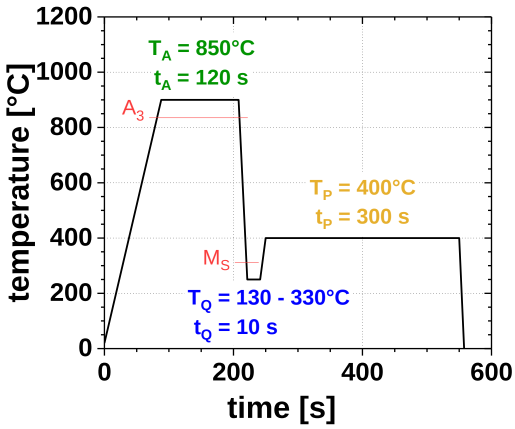

Figure 1. Schematic representation of the applied Quenching and Partitioning (Q&P) heat-treatment cycles for the investigated steels.

Tensile tests were performed according to DIN EN ISO 6892-1, using flat tensile specimens with 25 mm gauge length. For each heat-treatment condition, two samples were tested in a longitudinal direction. The microstructure was characterized by means of LOM using LePera etching. Furthermore, electrochemically polished samples were investigated by means of SEM using a Zeiss SUPRA 35 microscope (Carl Zeiss Microscopy GmbH, Jena, Germany). The volume fracture of RA was determined by means of SMM. Furthermore, interrupted tensile tests were performed at different strain levels to investigate the SIMT and thus, the RA-stability. By means of SMM, the RA-content at gradually increased strains was determined and finally the Ludwigson-Berger relation [19] was used to calculate the k_P-value as an indicator for the RA-stability.

$$\frac{1}{V_\gamma} - \frac{1}{V_{\gamma 0}} = \frac{k_P}{p} * \varepsilon^p \quad (1)$$

Here, V_γ is the volume fraction of RA determined at a specific true strain (ε), $V_{\gamma 0}$ is the initial RA-content before straining and k_P is a factor indicating the RA-stability. p is a strain exponent related to the autocatalytic effect of martensite formation, which can be considered as 1 for TRIP-steels, since this effect can be neglected close to RT [20].

The C-content in RA was determined by the application of the following equation proposed by Dyson and Holmes [21].

$$X_C = \frac{a_\gamma - 3.578 - 0.0056 * X_{Al} - 0.00095 * X_{Mn}}{0.033} \quad (2)$$

Here, X_C is the C-content in RA, a_γ is the austenite lattice parameter in Å, which was measured by X-ray diffraction (XRD) using a PANalytical XPert Pro diffractometer (Malvern Panalytical Ltd, Kassel, Germany) with Co-anode (λ = 0.179 nm, U = 35 kV). X_{Al} and X_{Mn} are the contents of Al and Mn in wt.% in RA, respectively, determined by energy dispersive X-ray spectroscopy (EDX, Carl Zeiss Microscopy GmbH, Jena, Germany).

3. Results

3.1. Transformation Behavior

Figure 2 depicts the dilatometer curves for the investigated steel grades quenched to 3 different T_Q, respectively. It is evident from the graphs that with increasing Mn-content, the M_S-temperature steadily decreased: for the steel grade containing 3.0 wt.% Mn (Figure 2a) the M_S-temperature of 333 °C was determined, for the Fe-C-3.5Mn-Si steel grade (Figure 2b) the M_S-temperature was 315 °C and for the steel grade containing 4.0 wt.% Mn (Figure 2c), an M_S-temperature of 305 °C was observed. Thus, in order to adjust a comparable amount of α'_{prim}, the increase of the Mn-content requires a lower T_Q. As a consequence, the illustrated T_Q were chosen in such a way that regardless of the chemical composition the red curves always correspond to a volume fraction of 50% α'_{prim}, the purple curves represent the samples containing of 75% α'_{prim}, and the blue lines depict the samples where 85% α'_{prim} was adjusted in the microstructure.

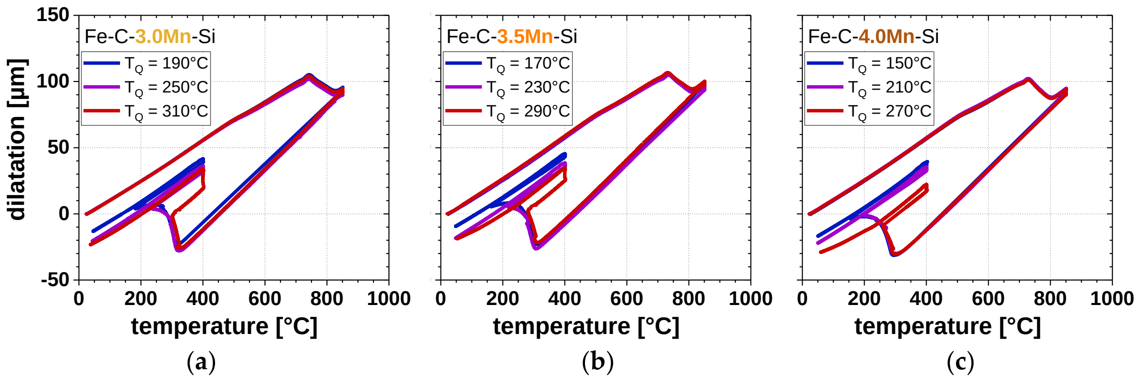

Figure 2. Dilatometric curves for the (**a**) Fe-C-3.0Mn-Si, (**b**) Fe-C-3.5Mn-Si, and (**c**) Fe-C-4.0Mn-Si steels quenched to different T_Q in order to adjust 50 vol.% (red), 75 vol.% (purple) and 85 vol.% (blue) α'_{prim}.

It is obvious from these dilatometric curves that during isothermal holding at T_P γ partially transformed to α_B, accompanied by a linear expansion. Figure 3 gives a detailed perspective on the dilatation during the partitioning step as a function of isothermal holding time. It is evident that with increasing T_Q, and thus decreasing volume fraction of α'_{prim}, a larger amount of α_B was formed. Irrespective of the chemical composition, for the samples with 75% and 85% α'_{prim} (purple and blue lines), rather comparable amount of α_B was formed, whereas for the samples with a matrix consisting of 50% α'_{prim} (red curve) a significant influence of the Mn-content on the formation of α_B could be stated: the higher the Mn-content, the lower the volume fraction of α_B.

In general, for all steels containing 50% α'_{prim}, the formation of α'_{final} was observed during cooling to RT (Figure 2). However, since with increasing Mn-content a decreasing amount of α_B was formed during the partitioning step, the largest volume fraction of α'_{final} was inherently formed for the steel grade containing 4.0 wt.% Mn.

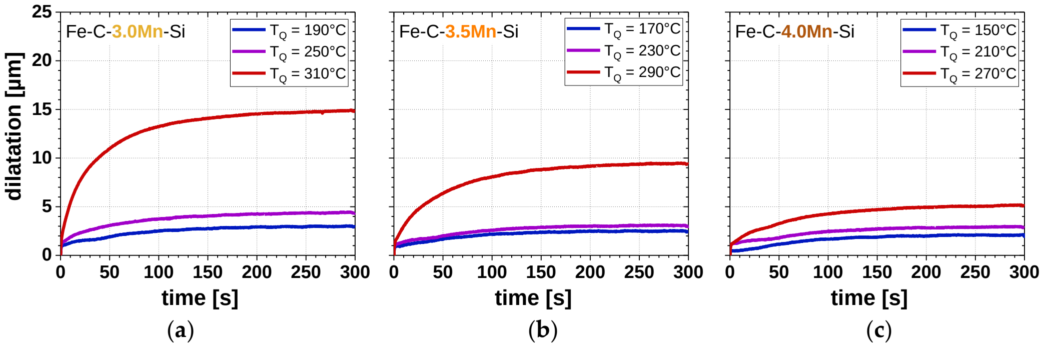

Figure 3. Dilatation due to formation of α_B as a function of isothermal holding time for the (**a**) Fe-C-3.0Mn-Si, (**b**) Fe-C-3.5Mn-Si and (**c**) Fe-C-4.0Mn-Si steels quenched to different T_Q in order to adjust 50 vol.% (red), 75 vol.% (purple), and 85 vol.% (blue) α'_{prim}.

3.2. Microstructure

Figure 4 depicts representative LOM (upper row) and SEM (lower row) images exemplarily shown for the Fe-C-3.5Mn-Si steel grade quenched to T_Q = 290 °C (Figure 4a,b), T_Q = 230 °C (Figure 4c,d), and T_Q = 170 °C (Figure 4e,f). During quenching into the M_S-M_f region α'_{prim} was formed, being subsequently tempered during isothermal holding at T_P. This lath-like carbon-depleted α'' partially included carbide precipitations visible in the SEM images. The microstructural investigation confirmed the results stemming from the analysis of the dilatometric curves, particularly the continuous increase in α'_{prim} and decrease in α_B fraction with declining T_Q. By means of SMM 18.5, 20.7 and 12.5 vol.%, finely distributed RA were measured for the samples quenched to 290, 230, and 170 °C, respectively. Owing to the extremely fine distribution of RA in the tempered-martensitic matrix, its localization is rather difficult using both LOM and SEM. It is obvious from the micrographs that for the sample quenched to 290 °C, a considerable amount of α'_{final} was present in the microstructure due to the insufficient chemical stabilization of austenite. This α'_{final} was characterized in the given microstructure observed by SEM by coarser and surface structured areas. For the steel grades containing 3.0 and 4.0 wt.% Mn, a similar influence of T_Q on the microstructural constituents could be confirmed using LOM and SEM. Regarding the influence of the chemical composition, no significant effect of Mn on the microstructural evolution could be observed at low T_Q, whereas for the higher T_Q, a larger volume fraction of α'_{final} was obtained for the Fe-C-4.0Mn-Si steel, as was also proved by the dilatometric measurements.

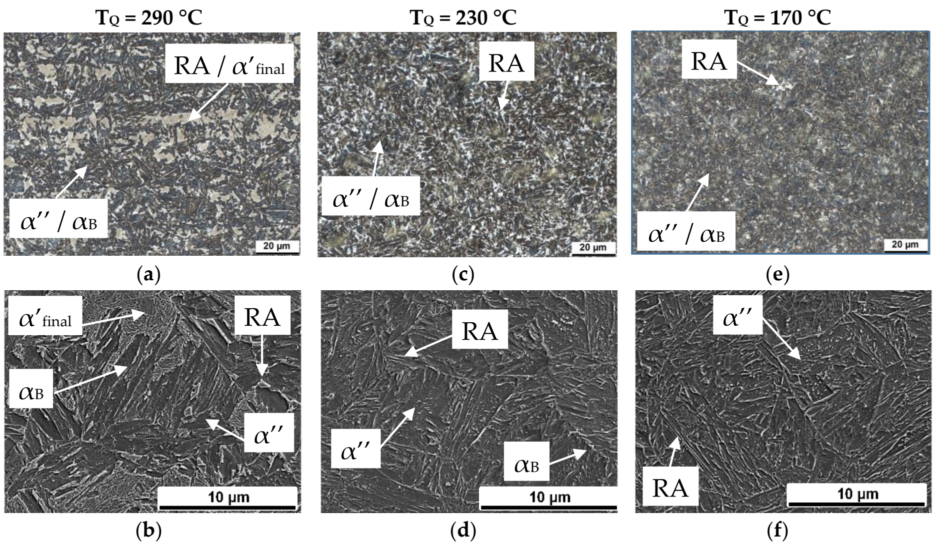

Figure 4. LOM and SEM micrographs of the Fe-C-3.5Mn-Si steel quenched to (**a**,**b**) T_Q = 290 °C, (**c**,**d**) T_Q = 230 °C and (**e**,**f**) T_Q = 170 °C.

Figure 5 summarizes the results obtained by dilatometry, microstructural investigations, and SMM for the three different steel grades, wherein the individual phase fractions of α″, α_B, RA and α'_{final} are plotted as a function of T_Q. Irrespective of the chemical composition, an increasing T_Q led to a remarkable decrease in the amount of α″, whereas the volume fraction of α_B simultaneously increased. Furthermore, the RA-content rose, until the specific T_Q where α'_{final} was formed as an aftermath of insufficient chemical RA stabilization. This inherently led to a decreasing volume fraction of RA with a further increase of T_Q. It can be regarded from the graphs that with an increasing Mn-content the volume fraction of α_B decreased, leading to a larger amount of RA. For the Fe-C-3.0Mn-Si steel the maximum RA-fraction (RA_{max}) of 19.9 vol.% was achieved at T_Q = 290 °C. For the steel grade containing 3.5 wt.% Mn RA_{max} = 22.3 vol.% was measured at T_Q = 270 °C, whereas by further increasing the Mn-content to 4.0 wt.% RA_{max} reached 24.6 vol.% at T_Q = 230 °C. These results indicate, that regardless of the chemical composition, the adjustment of approximately 70 vol.% α'_{prim} was necessary to stabilize the maximum volume fraction of RA. Thus, it can be inferred that the increase of the Mn-content requires the set of lower T_Q. In addition, the value of RA_{max} is positively influenced by an increasing Mn-content as a consequence of the lower fraction of α_B formed during the partitioning step.

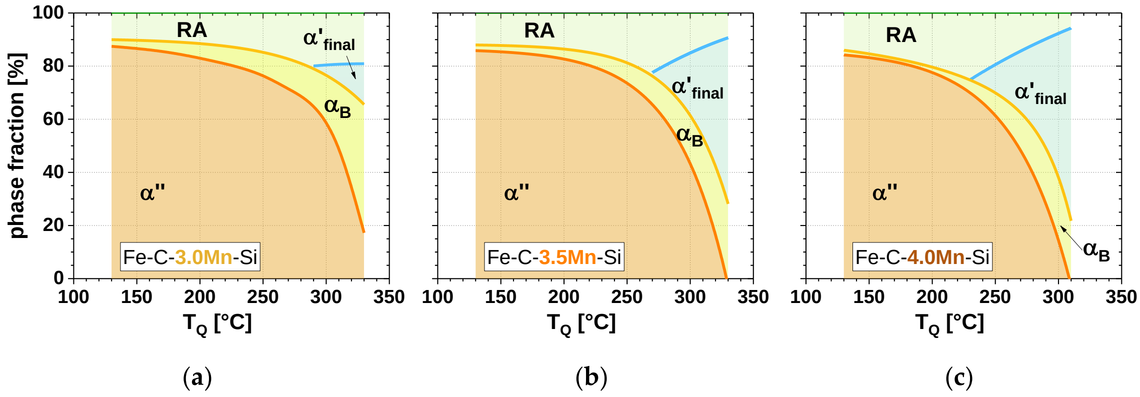

Figure 5. Phase fraction as a function of T_Q for the (**a**) Fe-C-3.0Mn-Si, (**b**) Fe-C-3.5Mn-Si, and (**c**) Fe-C-4.0Mn-Si steels.

3.3. Tensile Testing

Representative engineering stress-strain curves for the investigated steels are presented in Figure 6. For the samples containing approximately 85 vol.% α'_{prim} (blue curves) a comparable stress-strain behavior with very high yield strength (YS), low strain-hardening, and moderate TE was observed. In general, with increasing T_Q a significant decrease in YS was detected for all compositions. When increasing T_Q and thus adjusting 75 vol.% α'_{prim} (purple curves), UTS remained rather constant for the three investigated steels. However, in this case for all compositions an enhanced TE was obtained. When T_Q was further increased, which means that only 50 vol.% α'_{prim} (red curves) was present in the microstructure, a pronounced increase in UTS along with a remarkable decrease in TE was obtained. This was especially in case of the steels containing elevated Mn-contents. The presence of a considerable amount of α'_{final} in the microstructure was particularly responsible for this behavior.

Figures 7 and 8 depict the mechanical properties as a function of T_Q determined by tensile testing. It is clear that independent of the chemical composition first, with increasing T_Q both, YS and UTS decreased until reaching a T_Q of 230 °C (Fe-C-3.0Mn-Si), 210 °C (Fe-C-3.5Mn-Si), and 190 °C (Fe-C-4.0Mn-Si), respectively. This was associated with a decreasing amount of α'_{prim} and thus, increasing volume fraction of RA. Consistent with this, both UE and TE significantly increased, until reaching a sharp maximum, especially in case of the steels containing 3.5 and 4.0 wt.% Mn. Further rise of T_Q led to an increase in UTS, which was more pronounced for the steels with elevated Mn-contents. This was accompanied by a drastic reduction in both UE and TE. In contrast, for the Fe-C-3.0Mn-Si steel in the T_Q-range of 210–290 °C, a rather constant UTS and TE evolution could be obtained. This indicates that with increasing Mn-content, the sensitivity against T_Q fluctuations increased, leading to a narrower process window. Additionally, in case of the 3.5 and 4.0 wt.% Mn steels, at high T_Q, a rise in YS was noticeable, caused by the presence of considerable amounts of α'_{final} formed upon final cooling.

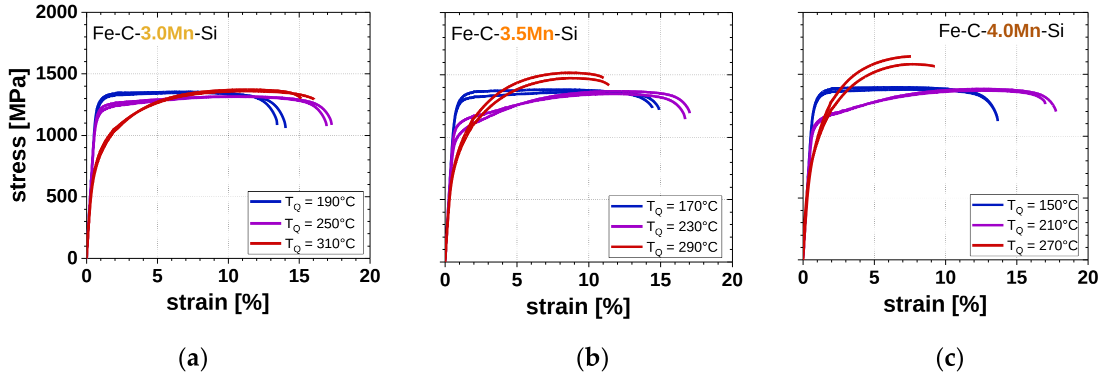

Figure 6. Stress-strain curves for the (**a**) Fe-C-3.0Mn-Si, (**b**) Fe-C-3.5Mn-Si and (**c**) Fe-C-4.0Mn-Si steels quenched to different T_Q in order to adjust 50 vol.% (red), 75 vol.% (purple) and 85 vol.% (blue) α'_{prim}.

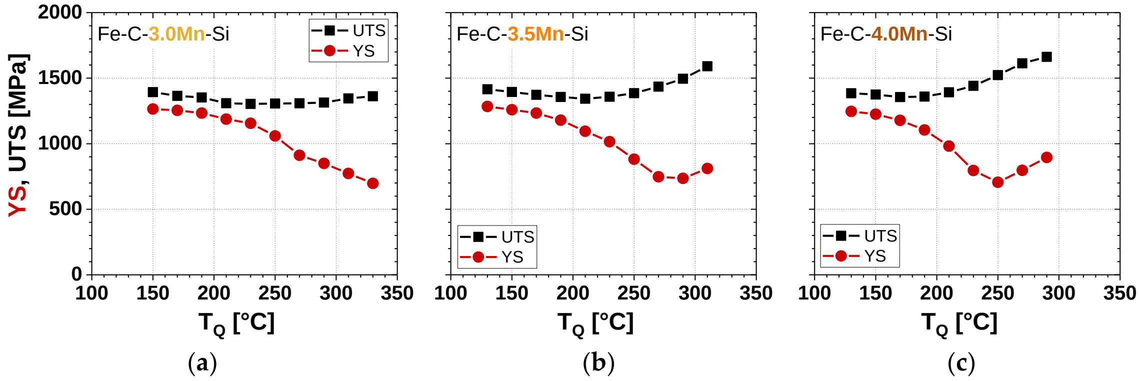

Figure 7. YS and UTS as a function of T_Q for the (**a**) Fe-C-3.0Mn-Si, (**b**) Fe-C-3.5Mn-Si and (**c**) Fe-C-4.0Mn-Si steels.

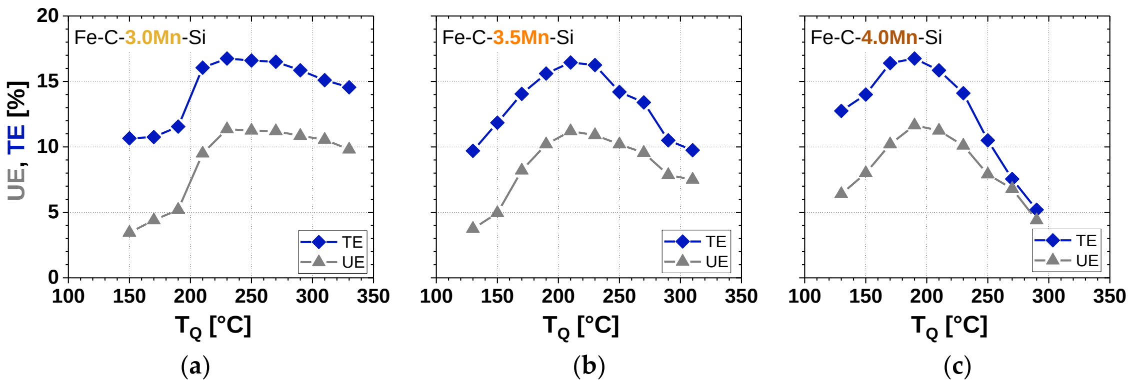

Figure 8. UE and TE as a function of T_Q for the (**a**) Fe-C-3.0Mn-Si, (**b**) Fe-C-3.5Mn-Si, and (**c**) Fe-C-4.0Mn-Si steels

Since the maximum TE was approximately 16.5% for all investigated steels, no evident influence of the Mn-content on the ductility of the investigated steels could be stated. Yet, with increasing Mn-content, a lower T_Q was necessary in order to adjust the maximum TE (T_Q = 230 °C, T_Q = 210 °C, and T_Q = 190 °C for the steels containing 3.0, 3.5, and 4.0 wt.% Mn, respectively). However, a slight influence of Mn on the strength was observed, since with increasing Mn-content UTS rose from 1304 MPa to 1343 MPa and 1360 MPa for the samples achieving the highest TE of 16.5%. Thereby, the best combination of strength and ductility was obtained for the Fe-C-4.0Mn-Si steel with a product of UTS × TE exceeding 22,500 MPa%.

3.4. Retained Austenite Stability

The volume fraction of RA in dependency of true strain is displayed in Figure 9. At a very low T_Q, where approximately 85 vol.% α'_{prim} was adjusted in the microstructure (blue curves), a rather moderate decline in RA-content was observed. This indicates a very stable RA that underwent only minor transformation during straining. The increase of T_Q led to a decline in α'_{prim} fraction to 75 vol.% (purple curves) and therefore to a higher initial volume fraction of RA. This contributed to the pronounced TRIP-effect under these conditions. However, for the samples containing only 50 vol.% α'_{prim} (red curves), a considerable amount of α'_{final} was present in the initial microstructure due to a very low chemical RA-stability. Therefore, in this case, a fast SIMT was observed, especially for the steel grades with elevated Mn-contents.

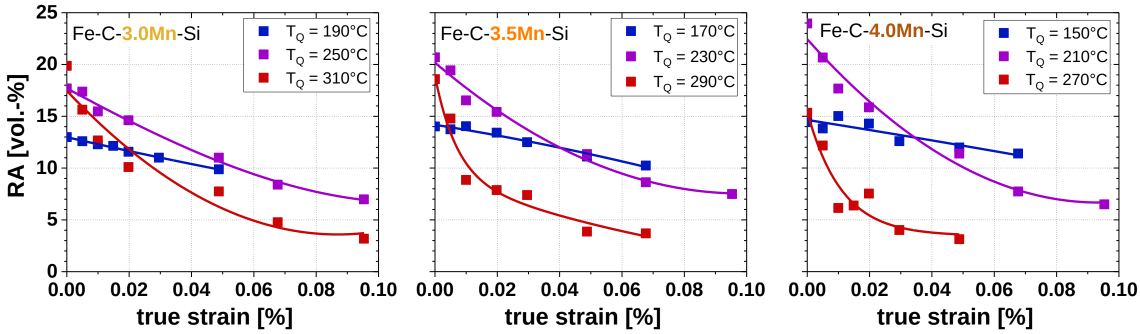

(**a**) (**b**) (**c**)

Figure 9. RA-content as a function of true strain obtained after interrupted tensile testing for the (**a**) Fe-C-3.0Mn-Si, (**b**) Fe-C-3.5Mn-Si and (**c**) Fe-C-4.0Mn-Si steels quenched to different T_Q in order to adjust 50 vol.% (red), 75 vol.% (purple) and 85 vol.% (blue) α'_{prim}

In order to enable a better comparison of the RA-stability of the individual steel grades, the volume fraction of γ transformed to α' is plotted as a function of true strain (Figure 10), following a linear relationship according to the Ludwigson-Berger equation (Equation (1)). With rising T_Q increasing k_P-values were observed, indicating a declining RA-stability. For the samples containing 85 vol.% α'_{prim} (blue curves) rather comparable k_P-values between 27 and 48 were determined for the investigated steels, whereas for the samples containing lower α'_{prim} fractions, a substantial influence of the chemical composition was observed. With increasing Mn-content, a significant decrease in RA-stability was found, represented by markedly increasing k_P-values.

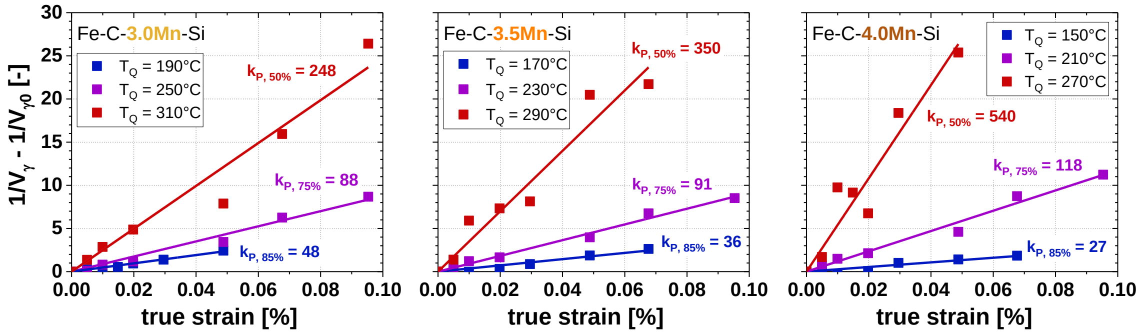

(**a**) (**b**) (**c**)

Figure 10. k_P-values indicating the RA-stability of the (**a**) Fe-C-3.0Mn-Si, (**b**) Fe-C-3.5Mn-Si and (**c**) Fe-C-4.0Mn-Si steels quenched to different T_Q in order to adjust 50 vol.% (blue), 75 vol.% (purple), and 85 vol.% (red) α'_{prim}.

In Figure 11a the k_P-values are plotted in dependence of T_Q, summarizing the results displayed in Figure 10. Regardless of the chemical composition, with increasing T_Q continuously rising k_P-values were observed. Since the Mn-content has significant influence on the M_S-temperature, the microstructure of the investigated steel grades consisted of different volume fractions of its individual constituents at comparable T_Q. For this reason, to ensure a better comparability of the steels, Figure 11b presents the k_P-values as a function of α'_{prim}. In general, with decreasing T_Q and hence increasing volume fractions of α'_{prim}, declining k_P-values were observed. This can be attributed to the decreasing fractions of γ_{remain} being present in the microstructure at the onset of the partitioning step. Thus, the C-content in the supersaturated α'_{prim} had to distribute to a lower volume fraction of γ_{remain}, leading to its enhanced stabilization. Furthermore, it is apparent from the graph that for the samples containing volume fractions of α'_{prim} exceeding 70 vol.%, the chemical composition rarely influenced the RA-stability. However, for the samples containing lower α'_{prim} fractions, the increase of the Mn-content led to a pronounced rise in k_P-values related to a substantial decline in RA-stability. The C-content in RA is displayed over the volume fraction of α'_{prim} in Figure 11c. For all steels, with increasing α'_{prim} fraction the C-content in RA rose. For the samples containing at least 70 vol.% α'_{prim} the increase of the Mn-content marginally influenced the C-content in RA. In contrast, at lower α'_{prim} fractions, the influence of the chemical composition was more remarkable, since a sharp decrease in C_γ was observed with increasing Mn-content.

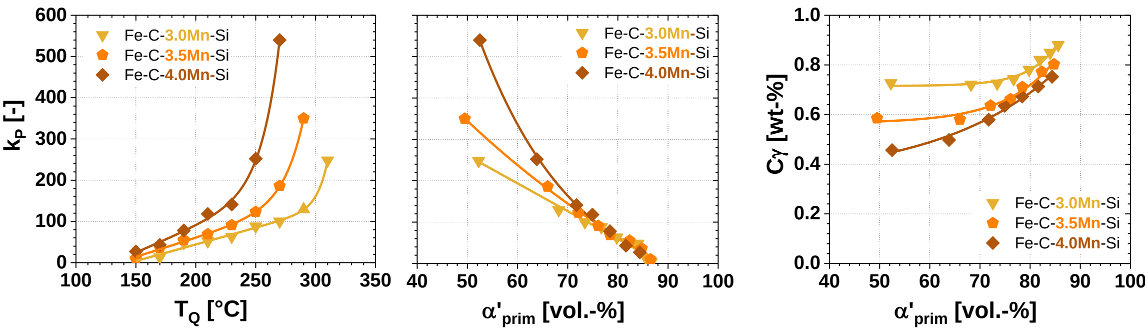

(**a**) (**b**) (**c**)

Figure 11. k_P-values indicating the RA-stability as a function of (**a**) T_Q and (**b**) α'_{prim}. (**c**) C-content in RA as a function of α'_{prim} for the investigated steels.

4. Discussion

4.1. Influence of Heat-Treatment Parameter

Regarding the influence of T_Q on the transformation behavior, the results presented in this contribution (Figures 2 and 3) could evidently confirm the findings already known for Q&P steels from the literature [22–25]. With an increasing T_Q, the volume fraction of α'_{prim} gradually decreased as a result of the reduced driving force for the $\gamma \rightarrow \alpha'$ transformation, as described by Koistinen and Marburger [26]. Coinciding with the decreasing amount of α'_{prim}, a larger volume fraction of γ_{remain} was present in the microstructure at the onset of isothermal holding at T_P. Hence, with a rising T_Q, a larger amount of γ_{remain} transformed to α_B. Furthermore, by increasing T_Q, a rising volume fraction of RA (Figure 5) was stabilized until exceeding a critical T_Q, leading to the formation of α'_{final} owing to the insufficient stabilization of γ_{remain}. Thus, in accordance with Speer et al. [27], a triangular shape of the RA-fraction as a function of T_Q could be observed (Figure 5).

The considerable influence of T_Q on the microstructural constituents obviously affected the mechanical properties of the investigated steels. With increasing T_Q, a decline in both UTS and YS accompanied by a rise in TE could be observed (Figures 6–8), which is consistent with the findings of De Moor et al. [12]. This behavior is linked to the decreasing volume fractions of α'_{prim} and in turn to rising RA-contents. Therefore, it is inferred that at very low T_Q, RA was hyper-stable, i.e., it underwent almost no transformation during deformation (Figures 9–11). With increasing T_Q the chemical RA-stability decreased (Figure 11c), resulting in a pronounced TRIP-effect, which contributed to the enhanced combination of strength and ductility. Independent of the chemical composition, the best combination of UTS and TE was observed 40 °C below a T_Q amount where the maximum RA-content could be stabilized at RT (T_Q = 230 °C, 210 °C, and 190 °C for the steels containing 3.0, 3.5, and 4.0 wt.% Mn, respectively). At a higher T_Q than the optimal one, a significant increase in UTS associated with a sharp decline in TE was observed, resulting in a remarkable deterioration of UTS × TE. This was linked to the presence of α'_{prim} in the initial microstructure related to low chemical RA-stability. Therefore, in this case, RA could not contribute to the enhanced TRIP-effect, which is in correlation with results reported in literature [28–30].

4.2. Influence of Mn-Content

Concerning the main topic of this contribution, the influence of the Mn-content on microstructure and resulting mechanical properties, interesting findings could be observed. First, the effect of an increasing Mn-content on the decrease in M_S-temperature reported in literature [31,32] was confirmed by means of dilatometry. Therefore, for the steels containing elevated Mn-content, lower T_Q were necessary in order to adjust comparable amounts of α'_{prim} (Figure 2).

In the case of the samples containing at least 80 vol.% α'_{prim}, only very low volume fractions of α_B were formed during isothermal holding at T_P. The increase of the Mn-content from 3.0 to 3.5 led to a slight decrease in volume fraction of α_B, and thus to a minor increase in RA-content (Figure 12a). These marginal differences in microstructure were directly reflected in the mechanical properties of the Fe-C-3.0Mn-Si and Fe-C-3.5Mn-Si steels, since the slightly increased volume fractions of RA contributed to a more pronounced TRIP-effect. As a consequence, a slight rise in UTS × TE was observed by increasing the Mn-content from 3.0 to 3.5 wt.% (Figure 12b) for the samples containing at least 80 vol.% α'_{prim}. Regarding the RA-stability, almost no differences in k_P-values were measured for these samples (Figures 10 and 11b). In counterpart, at comparable volume fractions of α'_{prim}, the C-content in RA shown in Figure 11c) was slightly lower for the steel containing 3.5 wt.% Mn, compared to the Fe-C-3.0Mn-Si steel grade. This could be attributed to the marginally larger RA-contents, leading to a lower C-enrichment during partitioning. In this context, higher products of RA-fraction and C-content in RA were achieved by an increase of the Mn-content from 3.0 to 3.5 wt.% (Figure 12c). On the contrary, the further increase of the Mn-content from 3.5 to 4.0 wt.% barely influenced the volume fraction of RA (Figure 12a). Therefore, the mechanical properties (Figure 12b) as well as the product of C_γ and RA (Figure 12c) remained almost unchanged.

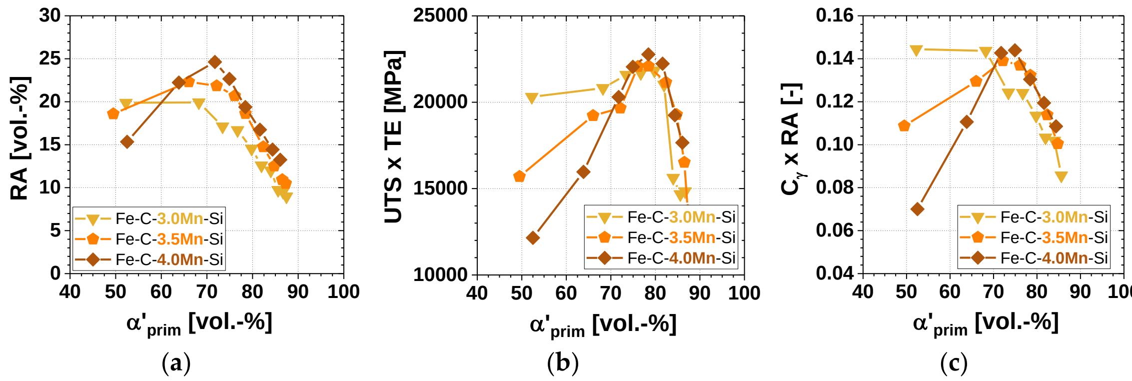

Figure 12. (**a**) RA-content, (**b**) UTS × TE and (**c**) C_γ × RA as a function of α'_{prim} for the investigated steels.

In general, in case of the samples containing at least 80 vol.% α'_{prim}, the C-diffusion from the supersaturated α'_{prim} to the γ_{remain} was the predominant mechanism for RA-stabilization. In contrast, the formation of α_B barely contributed to the C-enrichment of γ_{remain} due to its relatively low fraction. Furthermore, apart from the C-content in RA, its chemical stability is improved by an increased Mn-content in RA, as well. Since no evident Mn-parititoning during isothermal holding at T_P was observed by means of EDX, the higher Mn-content in the bulk composition counterbalanced the lower C_γ and inherently enhanced the chemical RA-stability for the steels containing 3.5 and 4.0 wt.% Mn. Nevertheless, it has to be considered that Mn influences the carbide formation in steels, since Mn is soluble in cementite [33]. This could lead to the precipitation of larger amounts of carbides during heat-treatment with increasing Mn-content, acting as carbon sinks and thus reducing the capacity for partitioning of C into γ. Hence, further research efforts are necessary to investigate the influence of Mn on the carbide precipitation and as a consequence C partitioning from the supersaturated α'_{prim} to γ_{remain} in the case of the present steels.

For the samples quenched to higher T_Q, in order to adjust 70–80 vol.% α'_{prim}, the influence of Mn on the phase transformation was more apparent compared to those containing higher fractions of α'_{prim}. This was due to the larger volume fractions of γ_{remain} being present at the onset of isothermal holding at T_P, influencing both the partitioning process and the formation of α_B. (Figures 2 and 3). According to the T_0-concept, a thermodynamic limit exists for the $\gamma \rightarrow \alpha$ transformation [34]. As γ_{remain} is enriched in C during the α_B formation, a diffusion-free transformation is thermodynamically impossible, as soon as the carbon content reaches a critical value. Since the difference in Gibb's free energy (ΔG_m) between γ and α is the driving force for the $\gamma \rightarrow \alpha$ transformation, the bainitic reaction stops if ΔG_m reaches 0 due to the C-enrichment in γ. This point is determined by the T_0-temperature. It is well known that Mn shifts the T_0-line to lower C-contents [35], allowing the formation of lower amounts of α_B in case of an increasing Mn-content owing to the above-mentioned thermodynamic limit. However, this effect is negligible compared to the general retarding effect of Mn on the bainitic transformation kinetics [36,37]. Mn enriches at the former austenitic grain boundaries, hindering the ferritic nucleation due to the local decrease in A_{e3}. In addition, Mn reduces the diffusion rate of C in γ, which has a clear retardation effect on the formation of α_B [38]. Therefore, in case of the samples containing 70–80 vol.% α'_{prim} the increase of the Mn-content led to lower fractions of α_B, and in turn to a significant rise in RA-content (Figure 12a). This increase in volume fraction of RA was accompanied by its decreasing chemical stabilization as proven by interrupted tensile tests (Figures 10 and 11), since the overall C-content had to partition to a larger volume fraction of γ_{remain}. Irrespective of the steel composition, the remarkably lower RA-stability compared to the samples quenched to lower T_Q contributed to the pronounced TRIP-effect, leading to enhanced strain hardening and thus improved combinations of UTS and TE (Figure 12b). Regarding the influence of the Mn-content, only minor differences in terms of mechanical properties could be found for these samples. This was linked to rather small deviations of $C_\gamma \times$ RA-content (Figure 12c), especially in the case of the samples containing 3.5 and 4.0 wt.% Mn.

However, for the samples containing even lower volume fractions of α'_{prim} (<70 vol.%), a substantial influence of the chemical composition on the phase transformation behavior and resulting structure-properties relation was found. In case of the Fe-C-3.0Mn-Si steel, the formation of up to 25 vol.% α_B (Figure 5) led to a moderate increase in RA-content along with decreasing α'_{prim} fractions. Since for the samples containing elevated Mn-contents the bainitic transformation was delayed, significant larger volume fractions of γ_{remain} transformed to α'_{final} during final cooling to RT, resulting in a sharp decrease in RA-contents with declining amounts of α'_{prim} (Figure 12a). In case of the Fe-C-3.0Mn-Si steel, this resulted in rather constant and high values of $C_\gamma \times$ RA (Figure 12c), whereas with increasing Mn-contents a drastic drop was observed, caused by the considerably declining RA-contents. Obviously, this was reflected in the stress-strain behavior of the investigated steels. For the composition containing 3.0 wt.% Mn, the mechanical properties remained almost unchanged by the increase of T_Q, resulting in almost consistent values of UTS × TE (Figure 12b). In contrast, for the Fe-C-3.5Mn-Si and Fe-C-4.0Mn-Si steels containing less than 70 vol.% α'_{prim}, the presence of α'_{final} related to very low RA-stabilities resulted in a significant increase in UTS, accompanied by a radical loss in TE. These results are coherent with those published by De Moor et al. [15] who reported a high sensitivity against T_Q-fluctuations in case of Q&P steels containing elevated Mn-contents. On that account, the formation of increased α_B fractions in case of the Fe-C-3.0Mn-Si steel contributed to the wider process window in terms of constant mechanical properties, compared to the steels containing 3.5 and 4.0 wt.% Mn.

5. Conclusions

This contribution focused on the study of the influence of the Mn-content on the microstructural evolution and mechanical properties of lean medium Mn Q&P steels containing 0.2% C, 1.5% Si, and 3.0–4.0 wt.% Mn, with a special emphasis on the RA-stability. The findings of the present paper are as follows:

- Regardless of the chemical composition, by increasing T_Q the volume fraction of α'_{prim} steadily decreased, accompanied by a rising amount of α_B and RA. The exceedance of a critical T_Q, depending on the Mn-content, resulted in an insufficient chemical stabilization of RA, triggering the formation of α'_{final} during final cooling to RT.
- A significant influence of the Mn-content on the phase transformation behavior could be observed, particularly with increasing T_Q and thus decreasing α'_{prim} fraction. The addition of enhanced Mn-contents led to an appreciable delay in $\gamma \rightarrow \alpha_B$ transformation during the partitioning step. Thus, on the one hand, larger volume fractions of RA could be stabilized with increasing Mn-content. On the other hand, the increase of the Mn-content adversely affected the RA-stability due to the declining C-content in RA, which was only partially counterbalanced by the enhanced Mn-content in RA.
- The mechanical properties achieved by the Q&P process were pronouncedly determined by both, volume fraction and stability of RA. With increasing Mn-content, a remarkably stronger sensitivity against T_Q-fluctuations in terms of RA-content and its stability was observed. As a result, the increase of the Mn-content resulted in a narrower process window with regard to the robustness of mechanical properties.
- For all investigated steels, the best combination of UTS and TE was observed for microstructures containing 75–80 vol.% α'_{prim}. For this reason, a T_Q 40 °C below the maximum RA-content had to be set in order to obtain the optimum mechanical properties. By increasing the Mn-content, the maximum value of UTS × TE could exceed 22,500 MPa%, since the larger volume fraction of RA by approximately 5% contributed to an enhanced TRIP-effect.

Author Contributions: Conceptualization, R.S., D.K., and C.S.; methodology, S.K.; software, S.K.; validation, D.K. and R.S.; formal analysis, S.K.; investigation, S.K.; resources, D.K., R.S., and S.K.; data curation, S.K., R.S., D.K., C.B., and C.S.; writing-original draft preparation, S.K.; writing-review and editing, R.S., D.K., C.B., and C.S.; visualization, S.K.; supervision, R.S., D.K., C.B., and C.S.; project administration, D.K., R.S., and C.S.; funding acquisition, D.K., R.S.

Funding: This research was funded by the Austrian Research Promotion Agency (FFG), grant number 860188, "Upscaling of medium Mn-TRIP steels".

Conflicts of Interest: The authors declare no conflict of interest. The funders had no role in the design of the study; in the collection, analyses, or interpretation of data; in the writing of the manuscript, or in the decision to publish the results.

Abbreviations

α	ferrite
α'	martensite
α'_{final}	final martensite
α'_{prim}	primary martensite
α''	tempered martensite
α_{B}	bainitic ferrite
a_γ	austenite lattice parameter
C_γ	carbon content in retained austenite
γ_{remain}	remaining austenite
ΔG_{m}	difference in Gibb's free energy
EDX	energy dispersive X-ray spectroscopy
k_P	factor indicating the RA-stability
LOM	light optical microscopy
MULTIPAS	multipurpose annealing simulator
p	strain exponent related to the autocatalytic effect
Q&P	quenching & partitioning
RA	retained austenite
$\mathrm{RA}_{\mathrm{max}}$	maximum retained austenite
RT	room temperature
SEM	scanning electron microscopy
SIMT	strain induced martensitic transformation
TE	total elongation
T_{P}	partitioning temperature
T_{Q}	quenching temperature
t_{Q}	quenching time
TRIP	transformation induced plasticity
UTS	ultimate tensile strength
$V_{\gamma 0}$	initial volume fraction of retained austenite
X_{Al}	aluminum content in retained austenite
X_C	carbon content in retained austenite
X_{Mn}	manganese content in retained austenite
XRD	X-ray diffraction
YS	yield strength

References

1. Fonstein, N. *Advanced High Strength Sheet Steels*, 1st ed.; Springer International Publishing: Cham, Switzerland, 2015; pp. 5–7.
2. Kwon, O.; Lee, K.; Kim, G.; Chin, K. New trends in advanced high strength steel - Developments for automotive application. *Mater. Sci. Forum* **2010**, *638–642*, 136–141. [CrossRef]
3. Steineder, K.; Krizan, D.; Schneider, R.; Béal, C.; Sommitsch, C. On the microstructural characteristics influencing the yielding behavior of ultra-fine grained medium-Mn steels. *Acta Mater.* **2017**, *139*, 39–50. [CrossRef]

4. Matlock, D.; Speer, J.; De Moor, E.; Gibbs, P. Recent developments in advanced high strength steels for automotive applications: An overview. *JESTECH* **2012**, *15*, 1–12.
5. De Cooman, B.C.; Speer, J. Quench and partitioning steel: A new AHSS concept for automotive anti-intrusion applications. *Steel Res. Int.* **2006**, *77*, 634–640. [CrossRef]
6. Steineder, K.; Krizan, D.; Schneider, R.; Béal, C.; Sommitsch, C. On the damage behavior of a 0.1C6Mn Medium-Mn Steel. *Steel Res. Int.* **2017**, *89*, 1700378. [CrossRef]
7. Steineder, K.; Schneider, R.; Krizan, D.; Béal, C.; Sommitsch, C. Comparative investigation of phase transformation behavior as a function of annealing temperature and cooling rate of two medium-Mn steels. *Steel Res. Int.* **2015**, *85*, 1–8. [CrossRef]
8. Arlazarov, A.; Gouné, M.; Bouaziz, O.; Hazotte, A.; Petitgand, G.; Berger, P. Evolution of microstructure and mechanical properties of medium Mn steels during double annealing. *Mater. Sci. Eng. A* **2012**, *542*, 31–39. [CrossRef]
9. Speer, J.; Matlock, D.; De Cooman, B.C.; Schroth, J. Carbon partitioning into austenite after martensite transformation. *Acta Mater.* **2003**, *51*, 2611–2622. [CrossRef]
10. Speer, J.; Aussuncao, F.; Matlock, D.; Edmonds, D. The quenching and partitioning process: Background and recent progress. *Mater. Res.* **2005**, *51*, 2611–2622. [CrossRef]
11. Owen, W. Effect of silicon on the kinetics of tempering. *Trans. ASM* **1954**, *46*, 812–829.
12. De Moor, E.; Lacroix, S.; Clarke, A.; Penning, J.; Speer, J. Effect of Retained Austenite Stabilized via Quench and Partitioning on the Strain Hardening of Martensitic Steels. *Metall. Mater. Trans. A* **2008**, *39A*, 2586–2595. [CrossRef]
13. Speich, G.; Leslie, W. Tempering of steel. *Metall. Trans.* **1972**, *3*, 1043–1054. [CrossRef]
14. Krauss, G. Tempering and structural change in ferrous martensitic structures. In *Phase Transformations in Ferrous Alloys: Proceedings of an International Conference, Proceedings of the International Conference on Phase Transformations in Ferrous Alloys, TMS-AIME, Warrendale, PA, USA, 1984*; Marder, A.R., Goldstein, J.I., Eds.; AIME: Englewood, CO, USA, 1984; pp. 101–123.
15. De Moor, E.; Speer, J.; Matlock, D.; Kwak, J.; Lee, S.-B. Effect of carbon and manganese on the quenching and partitioning response of CMnSi steels. *ISIJ Int.* **2011**, *51*, 137–144. [CrossRef]
16. De Moor, E.; Speer, J.; Matlock, D.; Kwak, J.-H.; Lee, S.-B. Quenching and partitioning of CMnSi steels containing elevated manganese levels. *Steel Res. Int.* **2012**, *83*, 322–327. [CrossRef]
17. Seo, E.-J.; Cho, L.; De Cooman, B.C. Application of quenching and partitioning processing to medium Mn steel. *Metall. Mater. Trans. A* **2015**, *46*, 27–31. [CrossRef]
18. Seo, E.-J.; Cho, L.; De Cooman, B.C. Kinetics of the partitioning of carbon and substitutional alloying elements during quenching and partitioning (Q&P) processing of medium Mn steel. *Acta Mater.* **2016**, *107*, 354–365.
19. Ludwigson, D.; Berger, J. Plastic behaviour of metastable austenitic stainless steels. *J. Iron Steel Inst.* **1969**, *207*, 63–69.
20. Matsumura, O.; Sakuma, Y.; Takechi, H. TRIP and its kinetic aspects in austempered 0.4C-1.5Si-0.8Mn steel. *Scr. Metall.* **1987**, *21*, 1301–1306. [CrossRef]
21. Dyson, D.; Holmes, B. Effect of alloying additions on the lattice parameter austenite. *J. Iron Steel Inst.* **1970**, *208*, 469–474.
22. Kaar, S.; Schneider, R.; Krizan, D.; Béal, C.; Sommitsch, C. Influence of the quenching and partitioning process on the transformation kinetics and hardness in a lean medium manganese TRIP steel. *Metals* **2019**, *9*, 353. [CrossRef]
23. Kaar, S.; Schneider, R.; Krizan, D.; Béal, C.; Sommitsch, C. Influence of the phase transformation behaviour on the microstructure and mechanical properties of a 4.5 wt.-% Mn Q&P steel. *HTM J. Heat Treatm. Mat.* **2010**, *74*, 70–83.
24. Santofimia, M.; Zhao, L.; Petrov, R.; Kwakernaak, C.; Sloof, W.; Sietsma, J. Microstructural development during the quenching and partitioning process in a newly designed low-carbon steel. *Acta Mater.* **2011**, *59*, 6059–6068. [CrossRef]
25. HajyAkbary, F.; Santofimia, M.; Sietsma, J. Optimizing mechanical properties of a 0.3C-1.5Si-3.5Mn quenched and partitioned steel. *Adv. Mater. Res.* **2014**, *829*, 100–104. [CrossRef]
26. Koistinen, D.; Marburger, R. A general equation prescribing the extent of the austenite-martensite transformation in pure iron-carbon alloys and plain carbon steels. *Acta Metall.* **1959**, *7*, 59–60. [CrossRef]

27. Speer, J.; Streicher, A.; Matlock, D.; Rizzo, F. Quenching and partitioning: A fundamentally new process to create high strength TRIP sheet microstructures. In Proceedings of the Austenite Formation and Decomposition MS&T, Chicago, IL, USA, 9–12 November 2003; pp. 505–522.
28. De Knijf, D.; Petrov, R.; Föjer, C.; Kestens, L. Effect of fresh martensite on the stability of retained austenite in quenching and partitioning steel. *Mater. Sci. Eng. A* **2014**, *615*, 107–115. [CrossRef]
29. Steineder, K.; Krizan, D.; Schneider, R.; Béal, C.; Sommitsch, C. The effects of intercritical annealing temperature and initial microstructure on the stability of retained austenite in a 0.1C-6Mn steel. *Mater. Sci. Forum* **2016**, *879*, 1847–1852. [CrossRef]
30. Seo, E.; Cho, L.; Estrin, Y.; De Cooman, B.C. Microstructure-mechanical properties relationships for quenching and partitioning (Q&P) processed steel. *Acta Mater.* **2016**, *113*, 124–139.
31. Mahieu, J.; Maki, J.; De Cooman, B.C.; Claessens, S. Phase transformation and mechanical properties of Si-free CMnAl transformation-induced plasticity-aided steel. *Metall. Mater. Trans. A* **2002**, *33*, 2573–2580. [CrossRef]
32. Schneider, R.; Steineder, K.; Watanebe, A.; Okumiya, M.; Krizan, D.; Sommitsch, C. Determination of a new empirical M_S-formula suitable for medium-Mn-steels. In Proceedings of the 24th IFHTSE Congress 2017—European Conference on Heat Treatment and Surface Engineering, Nice, France, 26–29 June 2017; pp. 1–9.
33. Satzinger, K. *Einfluss von Chrom und Mangan auf die Bainitbildung in Dualphasenstählen*; Diplomarbeit, Montanuniversität Leoben: Leoben, Austria, 2008.
34. Röthler, B. Möglichkeiten zur Beeinflussung der Mechanischen Eigenschaften von Kaltgewalzten TRIP-Stählen. Ph.D. Thesis, Technische Universität München, München, Germany, 2005.
35. Paul, S. Entwicklung Neuer Legierungskonzepte für Höchstfeste TRIP-Stähle mit Nicht Ferritischer Matrix und Reduziertem Siliziumgehalt. Ph.D. Thesis, Technische Universität München, München, Germany, 2012.
36. Eggbauer, G. Charakterisierung bainitischer Gefügezustände für Gesenkschmiedeteile. *BHM* **2014**, *159*, 5, 194–200.
37. Bleck, W.; Moeller, E. *Handbuch Stahl: Auswahl, Verarbeitung, Anwendung*, 1st ed.; Carl Hanser Verlag: Rastatt, Germany, 2017; pp. 292–293.
38. De Moor, E.; Matlock, D.; Speer, J.; Merwin, M. Austenite stabilization through manganese enrichment. *Scr. Mat.* **2011**, *64*, 185–188. [CrossRef]